FLOW THROUGH A COLLAPSIBLE TUBE

EXPERIMENTAL ANALYSIS AND MATHEMATICAL MODEL

ADOLPH I. KATZ, YU CHEN, *and* AUGUSTO H. MORENO

From the Departments of Civil Engineering, Mechanics and Materials Science, Rutgers University, New Brunswick, New Jersey 08903, and the Department of Surgery, Lenox Hill Hospital and New York University, New York 10021

ABSTRACT Flow through thin-wall axisymmetric tubes has long been of interest to physiologists. Analysis is complicated by the fact that such tubes will collapse when the transmural pressure (internal minus external pressure) is near zero. Because of the absence of any body of related knowledge in other sciences or engineering, previous workers have directed their efforts towards experimental studies of flow in collapsible tubes. More recently, some attention has been given towards analytical studies. Results of an extensive series of experiments show that the significant system parameter is transmural pressure. The cross-sectional area of the tube depends upon the transmural pressure, and changes in cross-section in turn affect the flow geometry. Based on experimental studies, a lumped parameter system model is proposed for the collapsible tube. The mathematical model is simulated on a hybrid computer. Experimental data were used to define the functional relationship between cross-sectional area and transmural pressure as well as the relation between the energy loss coefficient and cross-sectional area. Computer results confirm the validity of the model for both steady and transient flow conditions.

INTRODUCTION

One of physiologists' difficult concerns is the study of pressure-flow relationships in collapsible tubes transporting fluids to various sites inside or outside the body of living beings. Although any elastic tube will collapse when the surrounding radial forces are of sufficient magnitude to deform its walls, physiologists concentrate their interest in the case of thin-walled tubes which show regions of very small resistance to mechanical deformation. They refer to the walls of these tubes as being "structurally non-self-supporting" (1), meaning that when the tube is empty or when the pressure on its outside equals the pressure on its inside, the cross-section does not remain cylindrical as in more rigid tubes but flattens to an approximately elliptical configuration, i.e., the tube collapses. Conversely, filling the tube from the flat to the cylindrical configuration requires only a small change in inside pressure for a

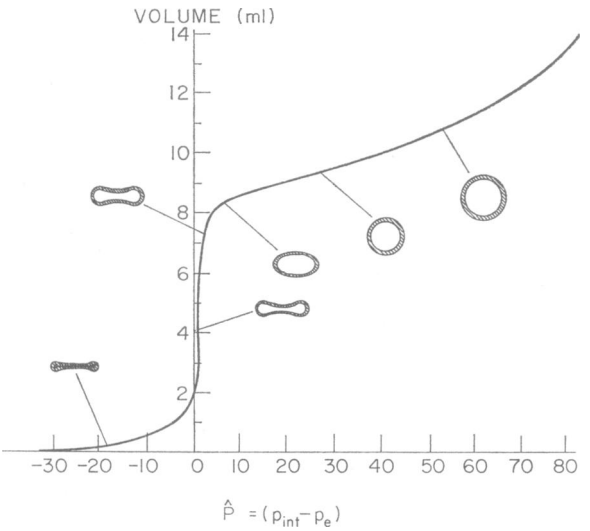

FIGURE 1 Volume in a collapsible tube as a function of transmural pressure. Typical transverse cross-sections are shown at various points on the curve.

relatively large change in volume (region of "free distensibility" [2]). Once the cross-section becomes cylindrical, considerably large changes in filling pressure produce only small further increments in volume. In this region the thin tube behaves as any other elastic tube resisting radial stretching as a function of the material properties of its walls (Fig. 1). Veins and certain segments of the airways of mammals are examples of such tubes. Because the pressure of the fluid flowing through these systems is of the same order of magnitude as that of the pressure surrounding the tubes, the concept of a transmural pressure or pressure difference across the wall of the tube (pressure inside minus pressure outside [3]) becomes increasingly meaningful. In the case of the veins, two additional factors complicate the study of the pressure-flow relationships. First, the veins traverse sealed regions or chambers of different surrounding pressure which include the thorax, the abdomen, and other tissue compartments. Second, the pressure in these chambers shows dynamic changes synchronous with respiratory and other body activities.

Physiologists studying the flow of fluids through veins and thin-walled flexible tubes uncovered flow characteristics drastically different from those of flow through more rigid elastic tubes such as arteries or from those of flow through rigid conduits. Unable to find rigorous treatments of these flows in the literature of physics and engineering they developed their own treatments frequently using analogies with phenomena of nature that included flow in rivers, dams, and other open channel systems. Some of the most significant studies include the works of Holt (4, 5), Duomarco (6, 7), Brecher (8), Rodbard (9, 10), Ryder and associates (2). Permutt and his coworkers (11, 12) proposed an algebraic approximation for the pressure-

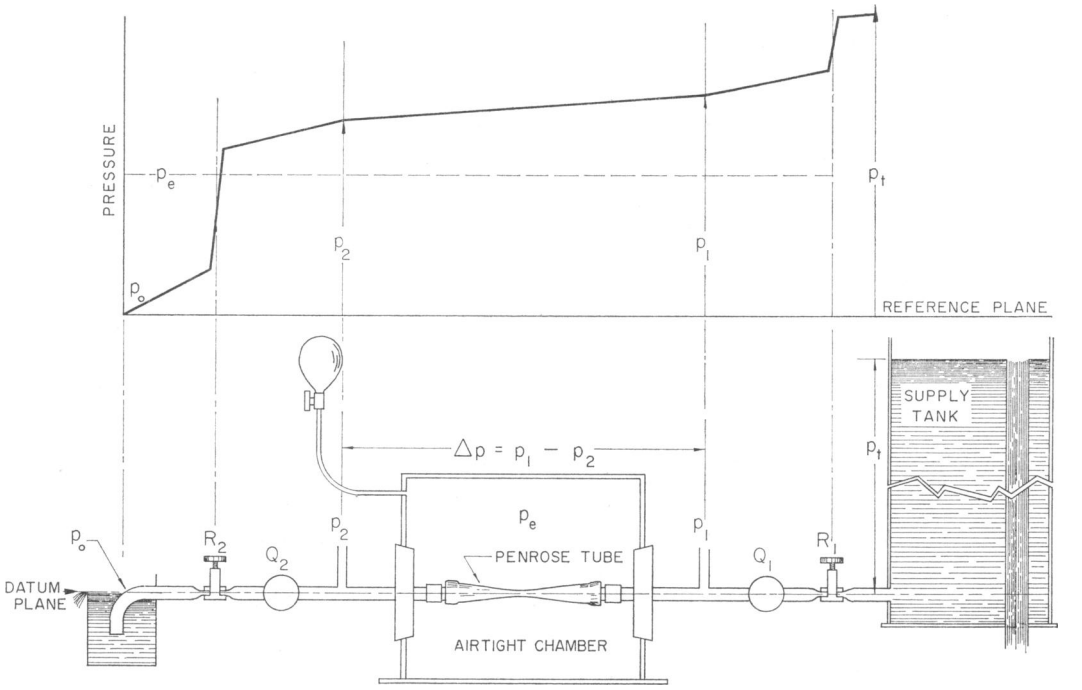

FIGURE 2 Schematic diagram of laboratory apparatus for the study of flow in collapsible tubes. R_1 and R_2 are adjustable orifices to control flow, Q, and pressure in the collapsible tube, p_e. A typical hydraulic gradient from the supply reservoir to the network outlet is shown above the diagram. Pressures measured by differential transformer type gauges and flows by electromagnetic flowmeters.

flow relationships based on the assumption of two different flow regimes, one when the tube is fully open and the other when it is fully collapsed (waterfall flow). Holt (4) introduced the most popular laboratory apparatus by interposing a segment of vein or thin-walled rubber tube in a rigid hydraulic network where the levels of a supply tank and an outlet reservoir regulated the pressure gradient for flow and a surrounding jacket provided an adjustable external pressure (Fig. 2). Many of the workers using this apparatus have followed traditional experimental methods in physiology, i.e., varying one pressure at a time while keeping the others constant. Some of the resulting information concerns particular cases rather than the general case of flow through thin-walled collapsible tubes. At any rate, the salient features of this information include: (*a*) increasing the hydraulic gradient by elevating the pressure in the supply tank augments the flow; however, increasing the gradient by lowering the outlet pressure may increase the flow, leave it unchanged, or even decrease it, depending on whether the tube remains open or collapses as a result of corresponding changes in transmural pressure; (b) the flow decreases with elevation of the pressure in the surrounding jacket; and (*c*) under certain conditions the tube

exhibits self-excited oscillations whose frequency and amplitude are functions of the elasticity of the wall, the flow rate through the tube, and the outlet pressure.

More rigorous treatments of flow through collapsible tubes include Fry's (13) analytical solution for steady flow which assumes that the dynamic terms are negligible and Kresch's (14) two-dimensional model for the change in cross-sectional area as a function of transmural pressure. Lambert (15), inspired by the experiments of Rodbard, developed the first simple mathematical model to predict average flow and oscillatory frequencies. In our laboratories we have conducted a systematic study of the problem using the apparatus of Holt. Essentially, we aimed to characterize the general pressure-flow relationships with families of curves obtained by varying one quantity at a time while letting the others seek their own values. These curves show that the pressure drop across the collapsible tube has a region of negative slope between two regions of positive slope (Fig. 3). One of our associates (16) has emphasized the concept of dynamic negative resistance implied in our curves. In this paper we take a different approach and present a mathematical model which predicts the general form of the experimental relationships. Our model is not a rigorous derivation from fundamental principles of continuum mechanics but rather a derivation from a careful analysis of our studies of flow through collapsible tubes.

EXPERIMENTAL STUDIES

In the apparatus of Fig. 2, the collapsible tube is a segment of thin-walled latex Penrose drain[1] (Davol Rubber Company, Providence, R.I.), 0.16 cm in thickness and 1.23 cm in diameter with a length to diameter ratio of 7:1 The collapsible tube maintains both a constant length and a constant cross-sectional area at each of its ends because it is held between two rigid tubes in the network. The surrounding airtight enclosure serves as a transparent chamber of adjustable external pressure.

We generate a typical pressure-flow curve (Fig. 3) by steadily changing the flow through the system while plotting the pressure drop across the collapsible tube ($\Delta p \equiv p_1 - p_2$) versus the volume flow rate (Q). Either changing the level of the supply tank (p_t) or varying the constriction of the upstream orifice (R_1) changes the flow in the manner required. The photographs show the progressive changes in longitudinal profile of the tube at different points along the curve. The sketches indicate the approximate configuration of its cross-sectional area at corresponding points.

The Δp-Q curve is a compact presentation of the relationship between the pressure gradient along the collapsible tube and flow. Together with the longitudinal and transverse profiles it displays considerable information related to the continuously changing transmural pressure, resistance, and geometry of the tube. In a less economic way we can gain more insight into the meaning of the curve by observing the individual variation of p_1 and p_2 within the hydraulic gradient in the network (Fig. 4). As we change the flow by varying the resistance of the upstream orifice (R_1), all pressures within the system change, including a pressure p_c located at some point between our points of measurement of p_1 and p_2 such that $p_2 < p_c < p_1$.

[1] Penrose drain or thin-walled soft rubber tubing used in the drainage of surgical wounds. It became popular as a mechanical analog for veins after its introduction by Holt.

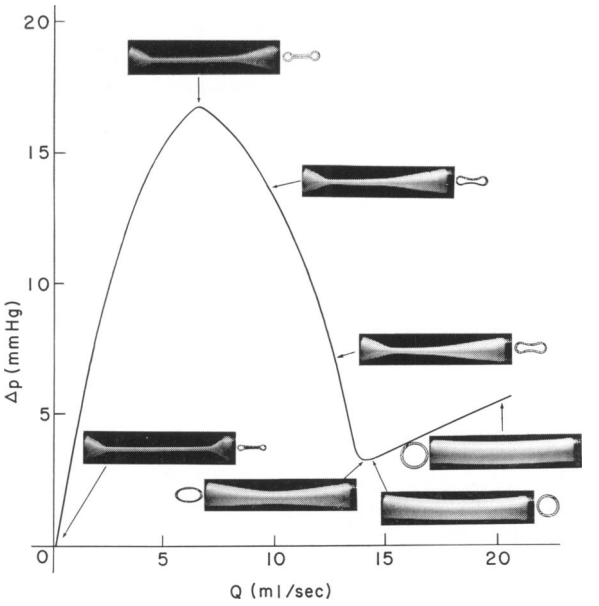

FIGURE 3 A typical pressure-flow curve for a collapsible tube. Δp is the pressure drop across the collapsible tube. Transverse and longitudinal cross-sections of the tube are shown for various Δp-Q states.

With large flows, p_c is greater than the external pressure (p_e), the tube reamins distended, and Δp is small. As flow decreases, p_c falls to eventually reach the value of p_e. At this point the tube begins to collapse and Δp increases rapidly. From then on small increments in R_1 markedly reduce the flow as the tube keeps collapsing and Δp keeps increasing. In this region p_1 remains nearly constant while p_2 decreases rapidly. With further reductions in flow, Δp decreases with Q until it reaches zero when flow ceases.

For a phenomenological characterization of the behavior of our system, we obtained first a family of Δp-Q curves by keeping the external pressure (p_e) constant for different settings of the downstream resistance (R_2). For convenience, we describe the curves from right to left, i.e., from higher to lower flows. Fig. 5 shows that for small values of R_2 the total resistance of the system is low and, because the pressure drop across R_2 is small, the pressure within the collapsible tube is nearly equal to the outlet pressure (p_o). Under these conditions, collapse begins at large values of Q. With higher values of R_2, the pressure within the collapsible tube increases and collapse begins at smaller values of Q. Since the pressure drop across the collapsible tube depends not only on the resistance of the collapsing tube itself but also on the flow through it, the maximum value of Δp decreases with an increasing R_2. With the smaller values of R_2, self-excited oscillations developed in the region of negative slope. It was always possible to find a critical value of R_2 that would eliminate the self-excited oscillations. We define the Δp-Q curve obtained with such limiting value of R_2 as the threshold curve.

Fixing the value of the downstream resistance (R_2) for different settings of the external pressure (p_e) resulted in a second family of curves (Fig. 6). With increasing p_e, collapse occurs at incrementally larger flows. Because of the combination of high resistance to flow and large values of flow, the value of maximum Δp increases with increasing p_e.

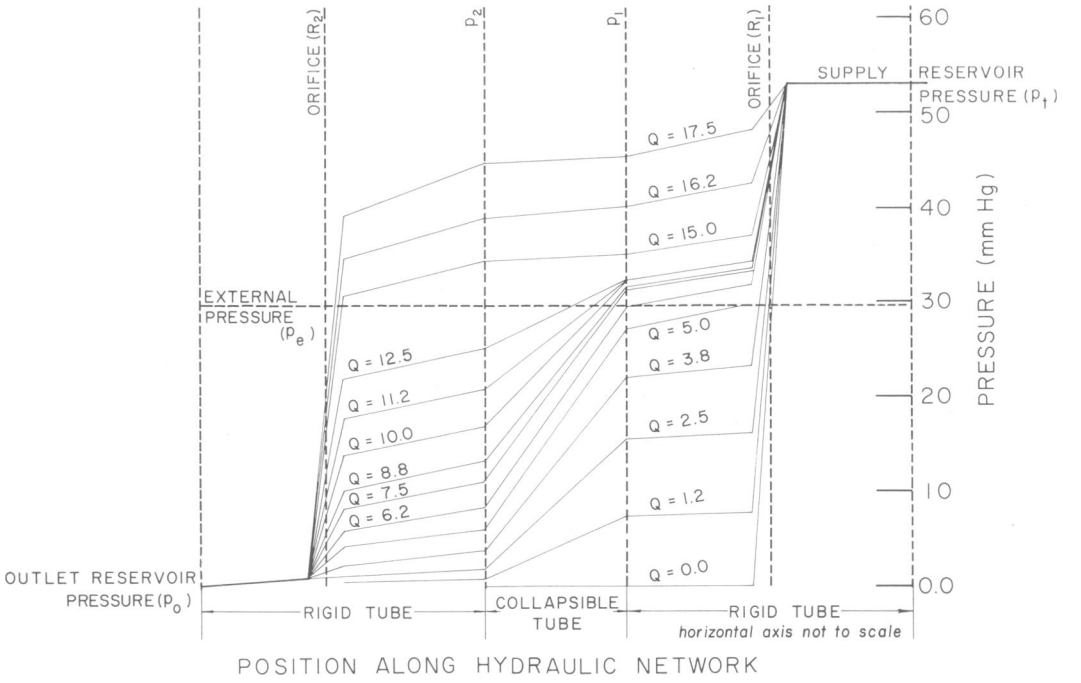

FIGURE 4 Hydraulic gradients along the network of experimental setup (Fig. 2) with flow, Q, as a parameter. Note the increase in Δp across the collapsible tube when the external pressure, p_e, is greater than the pressure within the tube.

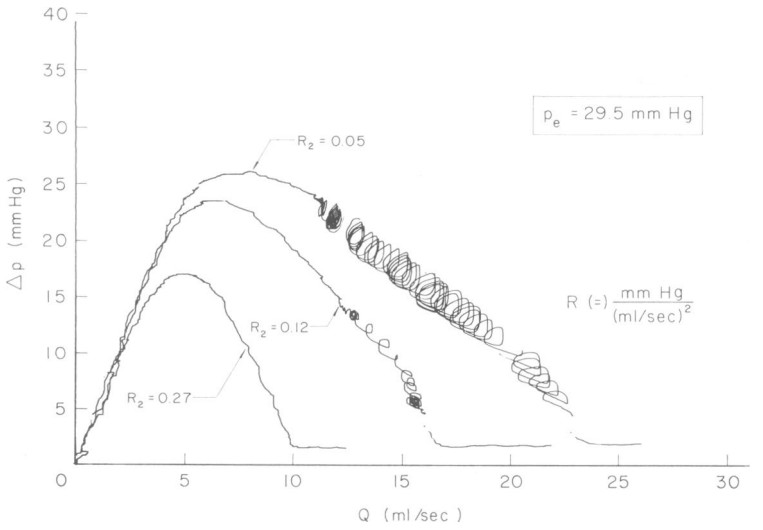

FIGURE 5 A family of experimental Δp-Q curves for flow in a collapsible tube with constant external pressure, p_e. The downstream orifice, R_2, is a parameter. Self-excited oscillations occurred for certain values of R_2 in the region of negative slope of the Δp-Q curve.

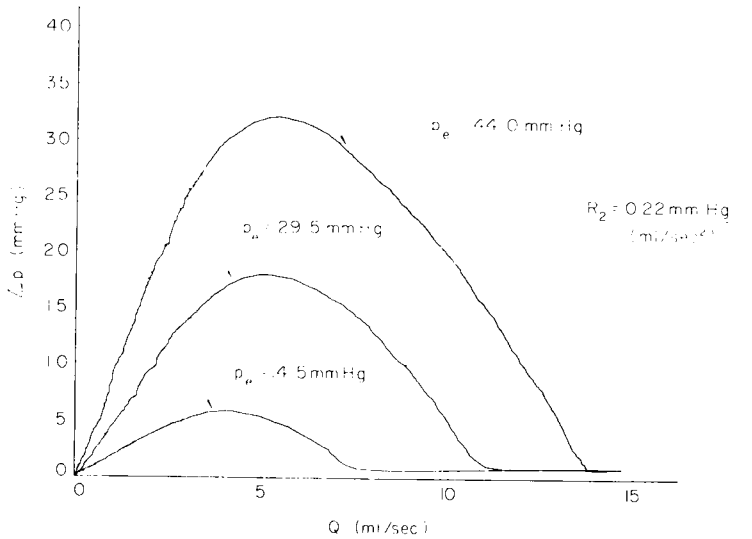

FIGURE 6 A family of Δp-Q curves for flow in a collapsible tube with a fixed downstream orifice, R_2. Ambient pressure, p_e, is a parameter.

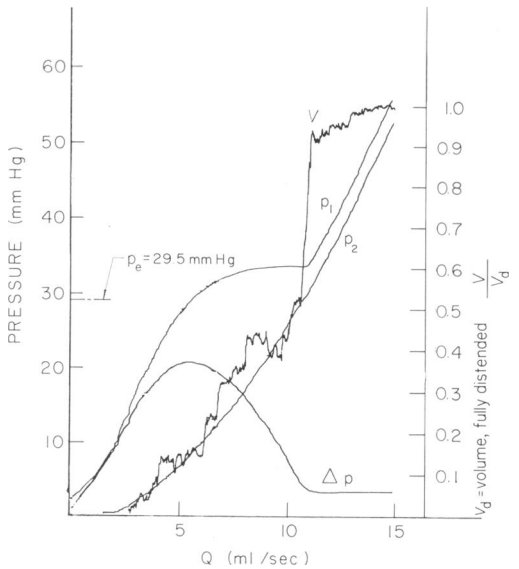

FIGURE 7 Volume, V, and pressure drop, Δp, as a function of flow in a collapsible tube. The pressure immediately upstream, p_1, and downstream, p_2, of the tube is also shown. Collapse is indicated by the sudden decrease in volume of the Penrose tube which occurs when the transmural pressure goes to zero.

As further characterization we give the simultaneous variation of p_1, p_2, Δp, and volume V as functions of Q (Fig. 7). We obtained the changing volume of the tube as a function of flow by extreme magnification of the minute changes in the pressure within the surrounding chamber.

Because the Δp-Q curves show that the volume flow rate Q is a multivalued function of the pressure drop Δp, we cannot predict the flow by knowledge of the pressure drop and

the parameters of the system, as we would in the case of a linear hydraulic network. In the collapsible tube we must not only know the pressure drop and the parameters of the system, but also the specific operating point of the collapsible tube. This is typical of a nonlinear system.

MATHEMATICAL MODEL

Fig. 8 is a schematic diagram of the model that we propose to describe the collapsible tube and the significant portions of the hydraulic network of Fig. 2. We assume a viscous and incompressible fluid. The collapsible tube consists of three segments: two compliant segments, BC and C'D, connected by a variable constriction segment, CC'. The rest of the model is comprised of two rigid segments AB and DE. We assume the flow to be quasi one-dimensional.

Since the collapsible tube segments upstream and downstream of the constricted section are short (less than 3 cm) and smooth, the pressure losses in them are negligible. These segments may be considered as regions of uniform pressure.

The cross-sectional area of the constriction is taken to be a function of the transmural pressure across the compliant upstream segment. The basis for this assumption is as follows: when the transmural pressures $\hat{P}_u$ and $\hat{P}_d$ are positive, the collapsible tube is fully open, and $\hat{P}_u \simeq \hat{P}_d$. When $\hat{P}_u$ and $\hat{P}_d$ approach zero, the tube begins to collapse. Hence the cross-sectional area in section CC' is a function of transmural pressure. Experimental results shown in Fig. 7 reveal that the pressure drop across the collapsed tube is small until the tube volume (and in turn, its cross-sectional area) reduces to about 40% of its original value. Hence, before collapse occurs it makes little difference whether we use $\hat{P}_u$ or $\hat{P}_d$ as the pressure controlling the cross-sectional area A_c. After the tube collapses, the pressure $\hat{P}_u$ will increase. When the absolute pressure upstream to the constriction becomes large enough to make the upstream transmural pressure positive, A_c will increase. Hence, it is reasonable to consider A_c as a function of $\hat{P}_u$.

Changes in cross-sectional area can occur in section BC, and flow can have components in the radial as well as the axial direction. By considering volumetric changes in the segment, however, the flow into and out of the segment will be one directional. To have a uniform pressure segment, we select the control volume for

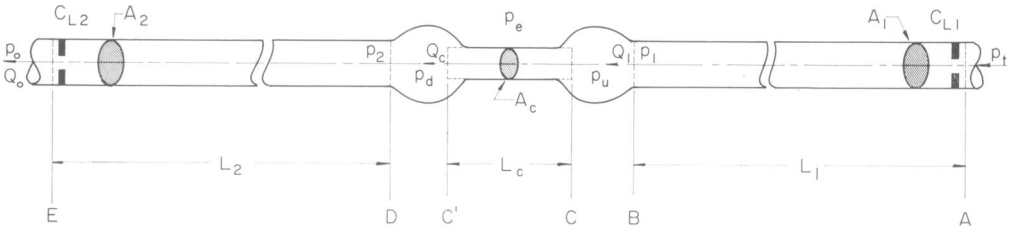

FIGURE 8 An idealized model for the collapsible tube in the hydraulic network of Fig. 2 (see text).

BC so that the inlet and outlet pressures are equal. The inlet to segment BC is the point where it connects to the thick wall tube AB. Locating the downstream boundary is more complicated and we will include it in the discussion for section CC'.

The continuity equation (conservation of mass) for the uniform pressure segment BC,

$$\frac{dV_u}{dt} = (Q_1 - Q_c) \tag{1}$$

where V_u is the volume of the segment and Q_1 and Q_c the volume flow rates for the rigid pipe AB, and the constricting segment CC', respectively. The volume of the collapsible tube is a function of the transmural pressure, $\hat{P}_u$, and therefore

$$\frac{dV_u}{dt} = C_u \frac{d\hat{P}_u}{dt} \tag{2}$$

where $C_u \equiv dV_u/d\hat{P}_u$ is the compliance of the segment. Substituting equation 2 into 1 yields a modified continuity equation

$$C_u \frac{d\hat{P}_u}{dt} = (Q_1 - Q_c) \tag{3}$$

where $\hat{P}_u$ is the transmural pressure across the segment wall,

$$\hat{P}_u = p_u - p_e . \tag{4}$$

Although in our experiments p_e was constant, for the more general case it can be a prescribed function of time.

We can write a similar continuity equation for segment C'D

$$C_d \frac{d\hat{P}_d}{dt} = (Q_c - Q_2) \tag{5}$$

where $\hat{P}_d$ is the transmural pressure for the segment, i.e.,

$$\hat{P}_d = p_d - p_e . \tag{6}$$

Because two axial boundaries, B and D, fix the flexible tube, collapse increases the length of its surface as the curvature of the surface goes from zero to a finite value. This increases the axial stress in the tube. The cross-section of the tube will change until the transverse components of axial stress are in equilibrium with the transmural pressure.

The V-$\hat{P}$ curve for a collapsible tube has the sigmoid shape in Fig. 2. We take the compliance in the segments BC and C'D as constants, and lump the nearly vertical portion of the V-$\hat{P}$ curve in the compliance for the central segment CC'. Since we

treat the segment CC′ as a cylinder, we can express its compliance in terms of the area, A_c.

Fig. 9 is a graph of cross-sectional area versus transmural pressure for the central section of the collapsible tube. This is the constitutive relation for the section CC′.

To develop the momentum equation for section CC′ we must define its control volume. Consider the constricted segment as a cylinder with a variable cross-section A_c, and constant length, L_c (Fig. 10). L_c is an "equivalent" length and can be estimated from experimental data. Upstream of CC′, the compliant segment BC is a reservoir with a uniform internal pressure p_u. On the downstream side, CC′ faces a reservoir, C′D, with uniform pressure p_d. We extend the control volume for the constriction into the upstream and downstream reservoirs until the end pressures of the control volume for CC′ are equal to p_u and p_d respectively. The dashed lines indicate the boundaries of the control volume in the direction normal to the flow. The wall of the tube is the lateral boundary of the control volume. For this control volume, we have momentum transport across the surfaces bf, ae, hd and gc as well as across the ab and cd faces which are normal to the axis of the tube. The axial momentum transport across the former surfaces will be small in comparison to

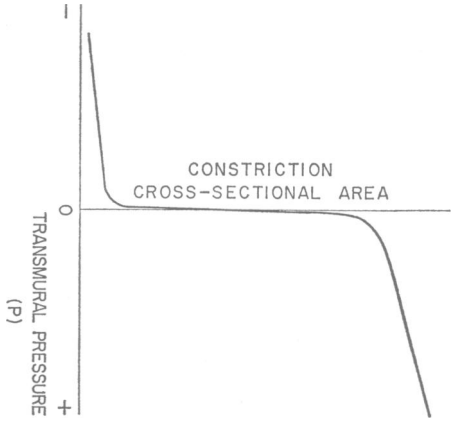

FIGURE 9 Transverse cross-sectional area at the center of a segment of collapsible tube as a function of transmural pressure.

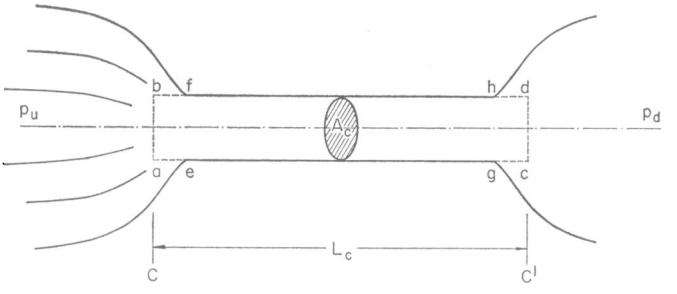

FIGURE 10 Control volume for the segment *CC′* of the collapsible tube model.

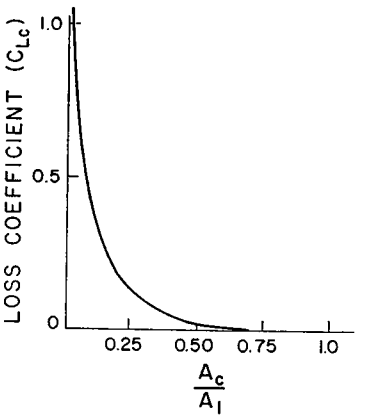

FIGURE 11 Energy loss coefficient, C_{L_c}, $(\Delta p = C_{L_c})[V^2/2g]$ for flow in converging-diverging section as a function of cross-sectional area, A_c/A_1.

the end faces for three reasons: (*a*) the axial component of velocity is small; (*b*) since the radial velocity is much smaller than the axial velocity, the rate of momentum transport into the control volume is small; and (*c*) the surface area is small.

The momentum balance for the control volume of Fig. 10 is

$$\frac{dQ_c}{dt} = (p_u - p_d)\frac{A_c}{\rho L_c} - \frac{C_{L_c} Q_c \mid Q_c \mid}{2L_c A_c} - \frac{8\pi\mu}{\rho A_c} Q_c. \tag{7}$$

The left-hand side of the equation represents the net momentum flux into the segment. The right-hand side contains the forces acting on the control element. The first term is the pressure force, the second is the resistance force due to change in geometry, and the third the losses due to the viscosity of the fluid.

Nonuniform flow occurs in the transition from the upstream compliant segment, BC′, through the constricted segment, CC′, to the downstream compliant segment, C′D. Analysis of flow through a converging-diverging section, similar to that of region BD for the collapsible tube, shows that the energy dissipation in the converging section, BD, is negligible (17). The loss coefficient C_{L_c} is therefore equal to the energy loss coefficient for the diverging flow. Analytical and experimental results (17) show that the relationship of C_{L_c} to A_c/A_1 is of the form in Fig. 11.

The resistance to flow in the rigid pipe segments is primarily due to the orifices corresponding to resistances R_1 and R_2. The momentum equations for these segments are therefore

$$\frac{dQ_1}{dt} = (p_t - p_u)\frac{A_1}{\rho L_1} - \frac{C_{L_1} Q_1 \mid Q_1 \mid}{2A_1 L_1} \tag{8}$$

and

$$\frac{dQ_2}{dt} = (p_d - p_o)\frac{A_2}{\rho L_2} - \frac{C_{L_2} Q_2 \mid Q_2 \mid}{2A_2 L_2} \tag{9}$$

where C_L is the orifice loss coefficient.

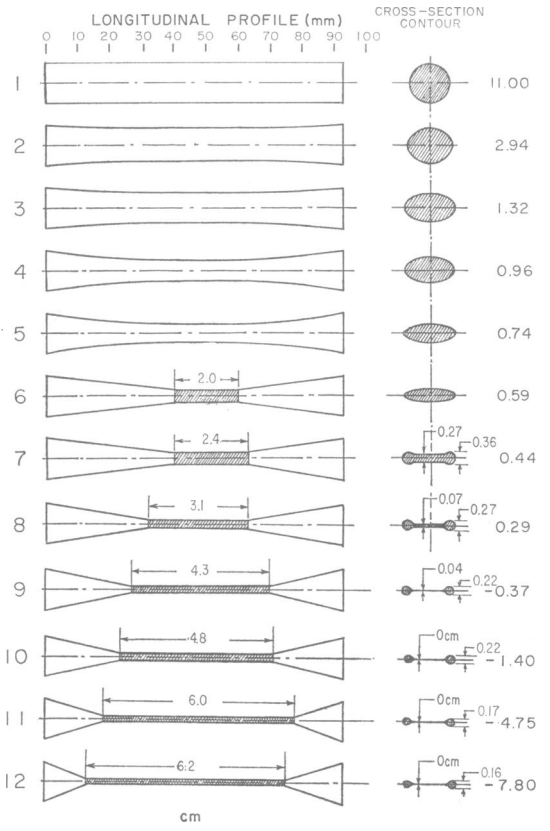

FIGURE 12 Measurements of longitudinal and transverse cross-sections of a collapsible tube segment at various transmural pressures.

We thus have seven equations (equations 3–9), and two empirical functions represented by Figs. 9 and 11 for the nine system variables, Q_1, Q_2, Q_c, $\hat{P}_u$, p_u, $\hat{P}_d$, p_d, A_c, and C_{L_c}, for the model of Fig. 8. There are ten system parameters, ρ, A_1, A_2, L_1, L_2, L_c, C_{L_1}, C_{L_2}, C_u, and C_d. With this model we can study both transient and steady-state flow in a collapsible tube.

We obtain C_{L_c} from the geometry of the collapsed tube after making transverse and longitudinal measurements over a range of transmural pressures (Fig. 12). We took the reference volume (V_0) for the collapsible tube at zero transmural pressure, $\hat{P} = 0$.

In addition to changes in the geometry of the tube, the loss coefficient, C_{L_c}, also depends on whether the flow is laminar or turbulent (18). To determine the flow regime we used the experimental results of Fig. 5. $R_2 = 0.12$. The Reynolds number for this case was always less than 2400.[2] Hence, it is reasonable to assume that the flow is laminar in the constriction as well as in the open tube.

[2] The Reynolds number, R_e, is defined as $R_e = \rho \bar{V} D/\mu$. D is the diameter of the tube. In some physiological work the radius is taken as the characteristic length. This results in a critical Reynolds number of 1200.

TABLE I

PARAMETERS, LOSS COEFFICIENTS, AND COMPUTED PRESSURE DROP ACROSS A COLLAPSIBLE TUBE ($A_1 = A_2 = 1.17$ cm²)

Q	A_c	A_1/A_c	C_{Lc}	V_c	$\rho \frac{V_c^2}{2} C_{L_c}$	L_c	$\frac{8\pi\mu LQ}{A_c^2}$	Δp	
ml/sec	*cm²*			*cm/sec*	*dynes/cm²*	*cm*	*dynes/cm²*	*dynes/cm²*	*mm Hg*
1	0.020	58.5	0.78	25.0	487	6.2	3875	4500	3.37
2	0.023	51.0	0.78	43.5	1476	6.2	5860	7336	5.50
3	0.025	46.6	0.78	60.0	2808	6.0	7210	10018	7.50
4	0.028	41.7	0.78	71.4	3976	6.0	7660	11636	8.73
5	0.031	37.8	0.77	80.6	5002	4.8	6240	11242	8.43
6	0.035	33.5	0.77	85.7	5655	4.8	5890	11545	8.66
7	0.038	30.8	0.76	92.1	6446	4.3	5210	11656	8.74
8	0.042	27.9	0.76	95.2	6887	4.3	4870	11758	8.82
9	0.045	26.0	0.75	100.	7500	4.3	4780	12280	9.21
10	0.049	23.9	0.68	102.	7074	3.3	3440	10515	7.89
11	0.053	22.1	0.55	104.	5949	3.3	3240	9189	6.90
12	0.057	20.5	0.50	105.	5512	3.1	2860	8373	6.29
13	0.08	14.6	0.42	162.	5523*	3.1	1572*	7095	5.32
14	0.16	7.3	0.33	87.	1249*	2.4	328*	1577	1.18
15	0.512	2.3	0.15	29.3	64*	2.4	34*	98	0.07

* Single lumen in tube—all other cases are for two cylindrical tubes as tube opening.

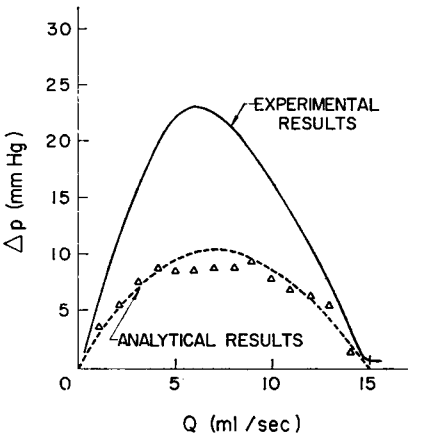

FIGURE 13 Analytical and experimental results for pressure drop, Δp, as a function of flow, Q, in a collapsible tube.

The loss factors, C_{L_c}, for the various tube profiles were obtained from the data of Albertson et al (19). Table I summarizes these computations.

Since the constricted tube has a finite length, we included the energy loss due to the viscosity of the fluid in determining the total head loss across the constriction.

Fig. 13 is a plot of the resulting analytical curve of Δp vs. Q. The scatter of points near the peak of the curve may relate to our difficulties in obtaining accurate measurements of the collapsible tube geometry. The resolution of the measurements was approximately 1.0 mm. A difference of 0.5 mm will nearly double the Poiseuille flow resistance in the collapsed tube and thereby increase by one-third the maximum Δp.

The difference between the analytical and experimental Δp peaks shown in Fig. 13 may be primarily due to three factors: (*a*) Accuracy of our measurements of the constricted section is limited. The values of A_c tend to be high resulting in low values of C_{L_c}. (*b*) The asymmetry of the actual constriction could result in a higher value for C_{L_c}. This is not accounted for in the simple theory for symmetrical constrictions. (*c*) High values of A_c result in lower values of Poiseuille resistance.

Nevertheless, the analytical results produce a Δp vs. Q curve that is similar in form to the experimental curve. The peaks of the two curves occur at virtually identical flow rates. The maximum value of the experimental curve is about twice the maximum value of Δp obtained from the model so we have the proper order of magnitude for C_{L_c}.

We conclude that the basic mechanism of the steady-state pressure-flow in a collapsed tube has been described. A reasonable estimate for the loss coefficient, C_{L_c}, in a collapsible tube can be established from the analysis of steady flow in a diverging nozzle.

COMPUTER SIMULATION OF COLLAPSIBLE TUBE

The mathematical model for the collapsible tube and the hydraulic network of Fig. 2 was programmed on an EAI 680 hybrid computer (Electronics Associates, Inc., Long Branch, N. J.).

We established the function for the cross-sectional area, $A_c = A_c(\bar{P}_u)$ from the results of the static test for cross-section geometry as a function of transmural pressure.

The loss coefficient function, $C_{L_c} = C_{L_c}(A_c)$ was based on the data of Table I.

Simple straight line approximations were made for A_c and C_{L_c} to simplify variation of parameters during simulation studies. A more elaborate representation would improve only the details of the results but would not change the general response. This was confirmed during computer studies.

To check the validity of the computer simulation for the collapsible tube, Δp vs. Q curves were obtained. The numerical values for the simulation parameters were obtained from the physical system used for experimental studies, Fig. 2.

In the experimental studies, the downstream resistance was

$$R_2 \equiv \frac{\Delta p_2}{Q|Q|} \tag{10}$$

where Δp_2 is the pressure drop across the downstream orifice. In the computer simulation the downstream resistance is

$$C_{r_2} = \frac{\Delta p}{\rho \bar{V}_2 |\bar{V}_2|/2} \tag{11}$$

where $\bar{V}_2$ is the average velocity for the transverse cross-section of the pipe.

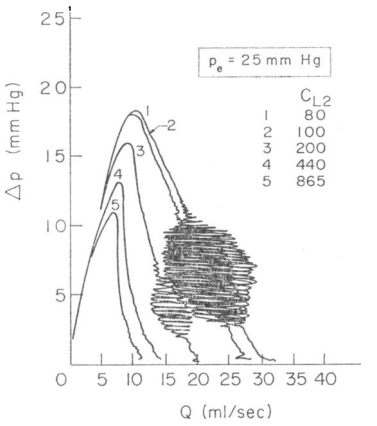

FIGURE 14 A family of Δp-Q curves obtained from computer simulation of flow in a collapsible tube with constant external pressure, p_e, and C_{L_2} as a parameter. (Compare with experimental results shown in Fig. 5.)

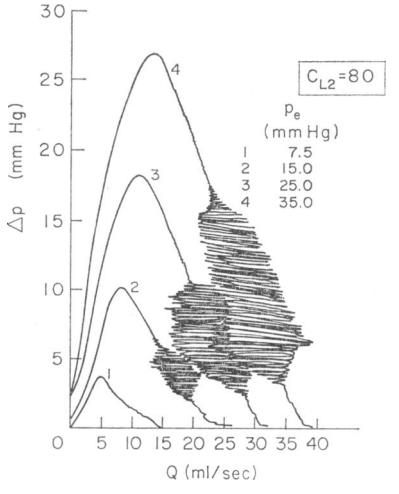

FIGURE 15 A family of Δp-Q curves obtained from computer simulation of flow in a collapsible tube with constant C_{L_2} and external pressure, p_e, as a parameter. (Compare with experimental results shown in Fig. 6.)

R_2 and C_{L_2} are related by

$$C_{L_2} = 2gA^2_{do}R_2 \tag{12}$$

in which A_{do} is the cross-sectional area of the downstream orifice. Since the magnitude of A_{do} is unknown, the value of C_{L_2} was adjusted on the computer to obtain a flow corresponding to the physical experiment. To decrease the flow in the system, the parameter C_{L_1} is increased to correspond to the experimental procedure of increasing R_1.

To have flow change from a maximum to zero for a specific value of R_2 in the

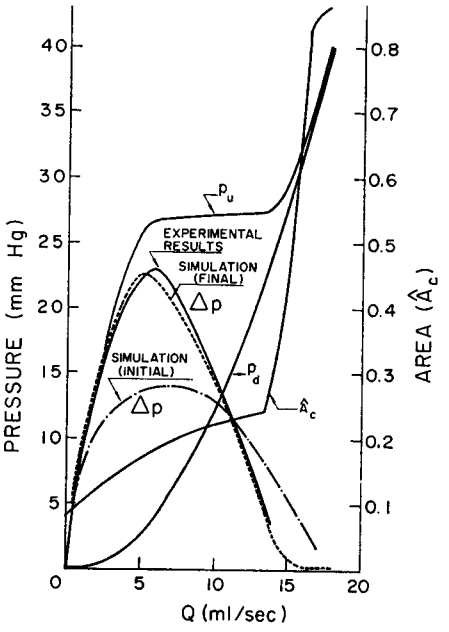

FIGURE 16 Simulation results for cross-sectional area, A_c, and pressure drop, Δp, as a function of flow in a collapsible tube. The variations of the Δp components, p_1 and p_2, are also shown. (Compare with Fig. 7.)

hydraulic network, R_1 was varied from zero to infinity. Because the range of the computer parameter C_{L_1} is limited, flow in the simulation was decreased by reducing the height of the supply reservoir. Both procedures produced the same results.

Simulation results for Δp vs. Q for constant external pressure, p_e, and variable downstream resistance, C_{L_2} are given in Fig. 14. These curves show good agreement with the experimental results of Fig. 5, for constant p_e and variable R_2. Increasing C_{L_2} results in a decrease of the peak Δp, the peaks are shifted to the left, and a threshold value for C_{L_2} can be attained.

In another simulation experiment C_{L_2} was held constant and the parameter, p_e, varied (Fig. 15). These results can be compared to the experimental results for constant R_2 and variable p_e shown in Fig. 6. In the experiment, however, the threshold value of R_2 was used. Again, simulation and experimental results agree. As in the experiments with increasing external pressure, p_e, the peak of the Δp vs. Q curve increases and shifts to the right.

To compare quantitatively the simulation and experimental results, and to check the magnitude of C_{L_c}, a simulation experiment was performed with $P_e = 29.5$ mm Hg. C_{L_2} was adjusted to initiate collapse at a flow rate of $Q = 15$ ml/sec corresponding to experimental results of Fig. 5, $R_2 = 0.12$. The resultant simulation curves together with the experimental results for Δp vs. Q are plotted in Fig. 16.

The peak of the simulation curve for Δp vs. Q was about one-half the maximum experimental value. We have already noted above that there is an uncertainty associated with the parameters C_{L_c} and A_c due to limitations both in analysis of non-

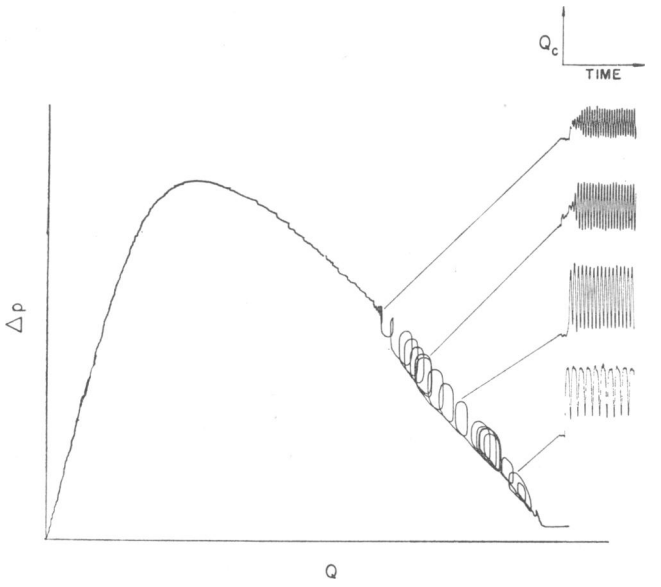

FIGURE 17 Experimental results showing buildup of self-excited oscillations in a collapsible tube at various points on the Δp-Q curve.

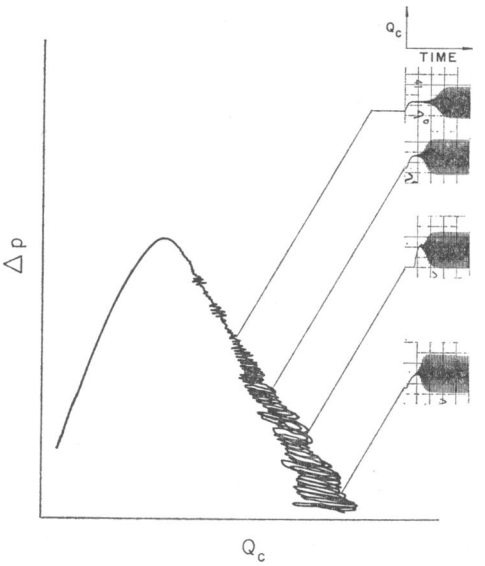

FIGURE 18 Simulation results showing buildup of self-excited oscillations in a collapsible tube at various points on the Δp-Q curve.

uniform flow and in obtaining measurements of the collapsed tube. Improvements in defining both of these parameters would tend to increase the peak of the Δp-Q curve and thereby more closely approximate experimental results. To match the experimental results it was necessary to increase C_{L_c} in the simulation by a factor of 10. Further refinements in determining both C_{L_c} and A_c are highly desirable.

The pressures p_u, p_d, and p_t, and the area A_c as functions of the flow rate are also plotted in Fig. 16. Reference to Fig. 7 indicates excellent correlation to experimental data.

The magnitude of instability is demonstrated by allowing oscillations to build up from an initial pressure-flow state at various points on the Δp vs. Q curve. Experimental results for this study are shown in Fig. 17. Both experimental and simulation results (Fig. 18) show that the relaxation oscillations build up rapidly at the initiation of collapse. As Q is decreased, the time to reach a stable level of oscillation is increased, and the amplitude of relaxation oscillations decrease.

CONCLUSION

Simulation results confirm the validity of the mathematical model of the collapsible tube for both steady state and oscillatory response. The simplicity of the model makes it suitable for inclusion as the collapsible segment for the physical model of the inferior vena cava (17, 20, 21), provided that one considers the differences between the fluid phases surrounding our collapsible tube and those surrounding the veins. Numerical values for model parameters can be derived from the dimensions and physical properties of the experimental system.

A limitation exists in determining the value of the loss coefficient C_{L_c}. The analytical value of C_{L_c} had to be increased by a factor of ten to obtain simulation results that were equal to the experimental values for maximum Δp. Thus, an order of magnitude increase can be expected for the analytical value of C_{L_c} for the collapsible inferior vena cava segment. Further study of energy dissipation in a collapsible tube would be necessary in order to derive a more accurate analytical expression for C_{L_c}.

NOTATION

A_1 cross-sectional area of pipe segment AB (cm^2)
A_2 cross-sectional area of pipe segment DE (cm^2)
A_c cross-sectional area of constriction (cm^2)
C_d compliance of segment downstream of constriction ($ml/[dyne/cm^2]$)
C_u compliance of segment upstream of constriction ($ml/[dyne/cm^2]$)
C_L head loss coefficient (dimensionless)
L length of segment (cm)
p_t pressure of supply tank ($dynes/cm^2$)
p_1 pressure downstream of 1st orifice, R_1 ($dynes/cm^2$)
p_u pressure upstream of constriction ($dynes/cm^2$)
p_c pressure in constriction ($dynes/cm^2$)
p_d pressure downstream of constriction ($dynes/cm^2$)
p_2 pressure upstream of 2nd orifice, R_2 ($dynes/cm^2$)
p_o outlet pressure ($dynes/cm^2$)
p_e external pressure ($dynes/cm^2$)
p_u transmural pressure across upstream compliant segment BC, $(= p_u - p_e)$ ($dynes/cm^2$)

$\hat{P}_d$ transmural pressure across downstream compliant segment C'D, ($= p_d - p_e$) (dynes/cm^2)
Q_1 volume flow rate through R_1 (ml/sec)
Q_c volume flow rate through constricted section (ml/sec)
Q_2 volume flow rate through R_2 (ml/sec)
R_1 resistance of upstream orifice
R_2 resistance of downstream orifice
r radial position (cm)
r_0 inside radius of tube (cm)
$\bar{V}$ space average velocity (cm/sec)
μ fluid viscosity (g/(cm/sec))
ρ mass density (g/cm^3)

Received for publication 11 March 1969.

REFERENCES

1. ALEXANDER, R. S. 1963. *In* Handbook of Physiology. Circulation. The American Physiological Society, Washington, D. C. **2**:1075.
2. RYDER, H. W., W. E. MOLLE, and E. B. FERRIS, JR. 1944. *J. Clin. Invest.* **23**:333.
3. BURTON, A. C., and S. YAMATA. 1951. *J. Appl. Physiol.* **4**:329.
4. HOLT, J. P. 1941. *Amer. J. Physiol.* **134**:292.
5. HOLT, J. P. 1943. *Amer. J. Physiol.* **136**:208.
6. DUOMARCO, J. L., and R. RIMINI. 1954. *Amer. J. Physiol.* **178**:215.
7. DUOMARCO, J. L., and R. RIMINI. 1962. *In* Cardiovascular Functions. A. A. Luisada, editor. McGraw-Hill Book Co., New York. 167.
8. BRECHER, G. A. 1956. Venous Return. Grune and Stratton, Inc., New York. 54.
9. RODBARD, S., and H. SAIKI. 1953. *Amer. Heart Journal.* **46**:715.
10. RODBARD, S. 1955. *Circulation.* **11**:280.
11. PERMUTT, S., and R. L. RILEY. 1963. *J. Appl. Physiol.* **18**:924.
12. PRIDE, J. B., S. PERMUTT, et al. 1967. *J. Appl. Physiol.* **23**:646.
13. FRY, D. L., and R. E. HYATT. 1960. *Amer. J. Med.* **29**:672.
14. KRESCH, E. 1968. Design of a Nonlinear Electrical Model for Veins. Ph.D. Thesis. University of Pennsylvania, Philadelphia.
15. LAMBERT, J. W. 1966. Proceedings of American Society of Civil Engineers, Engineering Mechanics Division Meeting, Washington, D.C.
16. CONRAD, W. 1969. *IEEE (Inst. Elec. Electron. Eng.) Trans. Bio-Med. Eng.* A. Noordergraaf and E. Kresch, editors. In press.
17. KATZ, A. I. 1968. A Model for the Dynamics of the Inferior Vena Cava of the Terrestrial Mammalian Cardiovascular System. Ph.D. Thesis. Rutgers University, New Brunswick.
18. KAYS, W. M. 1950. *Trans. ASME (Amer. Soc. Mech. Eng.). Ser. E: J. Appl. Mech.* **72**:8.
19. ALBERTSON, M. L., J. R. BARTON, and D. B. SIMONS. 1960. Fluid Mechanics for Engineers. Prentice-Hall International, Co., Englewood Cliffs. 290.
20. MORENO, A. H., and A. I. KATZ. 1968. Proc. Ann. Conf. Eng. Med. Biol.
21. MORENO, A. H., A. I. KATZ, and L. GOLD. 1969. Special Issue of *IEEE (Inst. Elec. Electron. Eng.) Trans. Bio-Med. Eng.* A. Noordergraaf and E. Kresch, editors. In press.